

J. Environ. Treat. Tech. ISSN: 2309-1185

Journal web link: http://www.jett.dormaj.com



# Yttria Stabilized Zirconia Thin Film as Solid Oxide Fuel Cell Electrolyte: Temperature Dependent Structures and Morphology

N. F. M. Rahimi 1\*, Sathiabama T. Thirugnana 2, S. K. Ghoshal 3

<sup>1</sup>Department of Physics, Faculty of Science, Universiti Teknologi Malaysia, 81310, Skudai, Johor, Malaysia 
<sup>2</sup>Razak Faculty of Technology and Informatics, Universiti Teknologi Malaysia, 54100, Kuala Lumpur, Malaysia 
<sup>3</sup>Department of Physics, Faculty of Science & Laser Centre, Universiti Teknologi Malaysia 81310, Skudai, Johor, Malaysia

Received: 23/10/2019 Accepted: 23/02/2020 Published: 20/05/2020

### Abstract

Fuel Cell is an electrochemical cell that supports clean and alternative energy that is mushrooming nowadays. Being a device of clean energy production, highly efficient solid oxide fuel cells (SOFCs) are increasing in demands. It converts the chemical energy into electrical energy in an environmentally-friendly way following green technology route. The SOFCs are one type of technology that has great promise to improve energy efficiency and to provide the society with clean and abundant energy. Yttria-stabilized zirconia (YSZ) is used as the electrolyte in SOFC wherein its synthesis with controlled properties is important to obtain the highest energy efficiency. The overall characteristics of the YSZ thin-film electrolyte in the SOFC are determined by its structures and morphologies. Based on these factors, a series of YSZ thin films were deposited on the sapphire wafer substrate by the dip-coating method and sintered in the temperature range of 900 – 1500 °C. The temperature dependent structural and morphological attributes of such thin films were determined and the prepared samples were characterized using XRD, AFM and Raman spectroscopy. The XRD patterns of the samples revealed the change in the crystallinity and phase, with an increase in the sintering temperatures while a tetragonal structure was observed at 1300 °C. Furthermore, the Raman spectral analyses supported the XRD results. The AFM morphology analysis of the thin films showed an increase in the grain size from 132.25 to 995.2 nm. The observed temperature-dependent changes in the structures and morphological attributes of these films may be useful for achieving high ionic conductivity required for an efficient SOFC construction.

Keywords: SOFC, Green technology, YSZ electrolyte, Thin film, Dip-coating, Structures, Morphology

## 1 Introduction

In recent years, generating highly efficient, clean, and environmentally-friendly sources of energy, energy carrier, and many more have become one of the biggest challenges for researchers, engineers, and prosumers. There are a lot of green technologies such as biomass, fuel cell and solar cell (1–3). One of the green technologies that have gained overall interest is fuel cell technology due to global warming that is now well underway due to the emission of flow out gasses, such as COx, NOx and so on (4). It is worrisome for future nature outcomes if this continues happening unchecked (5). Therefore, it is important to improve the properties of the YSZ electrolyte films useful for SOFCs. A fuel cell converts chemical energy to electrical energy in which no combustion is required during the process (6). In this paper, one of the fuel cell types called Solid Oxide Fuel Cell (SOFC) is presented. SOFC has the greatest potential of any fuel technology due to low-cost ceramic materials and high

electrical efficiencies (5). The most important part of SOFC is electrolyte as the subject itself uses solid ceramic materials as the electrolyte (7). Zirconia is widely used in a corrosive environment. Usually, it can be found in pipes, steel alloys, bricks, ceramic, and artificial gemstones. Zirconia is also utilised for catalytic converters. In other words, zirconia materials are very universal and widely used. Pure zirconia (ZrO<sub>2</sub>) is chosen as the electrolyte material for SOFC application as it has more advantages in terms of its properties, such as mechanical, optic, hardness, strength, and high ionic conductivity (8-10). At atmospheric pressure, ZrO<sub>2</sub> has three polymorphic structures between room temperature until its melting point is reached at 2826 °C, namely monoclinic, tetragonal, and cubic (3,11). At room temperature, the monoclinic structure is thermodynamically stable before turning tetragonal when it reaches 1170 °C. After that, above 2370 °C (12), a stable cubic structure is formed. However, the tetragonal and cubic structures can be

Corresponding author: N. F. M. Rahimi, Department of Physics, Faculty of Science, Universiti Teknologi Malaysia, 81310, Skudai, Johor, Malaysia. E-mail: fathirahrahimi@gmail.com.

stabilised at room temperature either by doping with cation covalent/trivalent as stabilisers (e.g. Y2O3, CaO, and MgO) or by lowering the crystallite size so that it can fix to more effective applications in various fields (13). In the SOFC system, a cubic structure is the most stable structure for electrolytes and performs the best and highest ionic conductivity functions due to its equal number number of vacant oxygen sites in all crystalline lattice directions. Among all dopants used to stabilise ZrO2, the most suitable type is Y<sub>2</sub>O<sub>3</sub> because of high oxygen ion conductivity. Yttria has the cubic form of rare earth oxide structure by itself according to the ordering of oxygen vacancies in the fluorite structure, along with the directions [111] (14). ZrO<sub>2</sub>-Y<sub>2</sub>O<sub>3</sub> or Yttria-stabilised zirconia (YSZ) is the cubic solid solution system, whereas tetragonal is also unexceptional because of both structures' desire to stabilise at a high temperature (15). When increasing the value of doping, the conductivity of YSZ will rise and reach the maximum, thus yielding many contributions in wide-ranging applications. It offers good properties such as high mechanical strength, good chemical stability, high level of oxygen-ion conductivity, and low thermal conductivity (16,17). The amount of yttrium doping is one of the parameters that must be controlled as it will later influence the grain size, martensite temperature, and strength properties. According to (11,18), 8mol% of doping yttrium show the highest ionic conductivity performance.

# 2 Materials and Experimentals

#### 2.1 Chemicals Materials

Chemicals acquired from Sigma Aldrich to deposit the YSZ films were Yttria-stabilised zirconia (IV) oxide, ethanol, and polyethylene glycol (PEG).

## 2.2 Instruments

The dip-coater machine (PTL-MM01) was used for the preparation of thin films. The hotplate (IKA C-MAG HS 7) and ultrasonic bath (BRANSON 3510) were also utilised.

# 2.3 YSZ thin films deposition

By mixing yttria-stabilised zirconia (IV) oxide (Sigma Aldrich, particle size below 100 nm) with PEG as the binder in a certain amount of ethanol, the suspension for dip coating was prepared. The mixture was stirred for 2 h on the hotplate at room temperature before subjected to the ultrasonic treatment for another 30 min. Sapphire wafer was used as the substrate, with a dimension of 1 cm × 1 cm. The samples were cleaned in the ultrasonic bath using ethanol followed by acetone before they were rinsed in distilled water and kept dry and clean before they could be used. The coating speed was fixed at 150 mm/s as each layer of the coating was prepared. The final process of sintering process was set for 900 °C, 1000 °C, 1300 °C, 1400 °C, and 1500 °C, resulting in the samples labelled as YSZ9, YSZ10, YSZ13, YSZ14, and YSZ15 respectively, based on the temperature used.

## 2.5 Samples Characterizations

The X-ray Diffractometer (Rigaku smartlab X-ray Diffractometer) With Cu K $\alpha$  radiation of wavelength,  $\lambda \approx 0.154$  nm) was used to analy se the structural characterization of thin films. The pattern of X-ray diffraction (XRD) was

recorded between 20 ° to 90 ° with the step size of 0.01°. Meanwhile, the Atomic Force Microscope (Nanowizard® 3 Atomic Force Microscope) was utilised to analyse the morphology, surface roughness, and thickness of the thin films. The image of the AFM was recorded with a scale of 3  $\mu m^2$ . Raman Spectrometer (UNIDRON Micro Raman Mapping System) was employed to measure the vibration bond and crystal structure of the thin films.

## 3 Results and Discussions

### 3.1 X-Ray Diffraction crystal phase analysis

Figure 1 shows the XRD patterns of the synthesised YSZ thin films with one coating layer sintered at different temperatures. The samples sintered at 900, 1000, 1300, 1400, and 1500 °C were named as YSZ9, YSZ10, YSZ13, YSZ14, and YSZ15, respectively. The peak appeared when the thin films were sintered at 1300 °C and above due to grain growth happening during the heating process. The XRD patterns revealed the tetragonal structure for YSZ13, YSZ14, and YSZ15 with the highest peak (101) corresponding to the tetragonal structure. The peak (101) increased from YSZ13 to YSZ14 and decreased at YSZ15. The change of crystal phase in the thin films is shown in Figure 2 by the shifting peak at (101) and its increasing intensity. The shifting showed that the stress and strain effect happened in the film growth during the heating process. The highest intensity indicated more crystallinity in the thin films accordingly (8). The crystallite size, strain and lattice parameter were shown in Table 1. The crystallite size was calculated by using Scherrer Formula where the full width at half maximum (FWHM) of the most intense diffraction peak was chosen:

$$D = \frac{k\lambda}{\beta \cos \theta} \tag{1}$$

where D is Crystallite Size, k is shape factor constant,  $\beta$  is FWHM,  $\theta$  is diffraction angle (in radians) and  $\lambda$  is wavelength of X-ray. The lattice strain,  $\epsilon$  was calculated by Williamson-Hall relation:

$$\varepsilon = \frac{\beta \cos \theta}{4} \tag{2}$$

In equation  $2\varepsilon$  is lattice strain. Last relation equation was used to find the lattice parameter of tetragonal YSZ:

$$\frac{1}{d^2} = \frac{h^2 + k^2}{a^2} + \frac{l^2}{c^2} \tag{3}$$

where d is lattice planer sapcing, h, k, and l is the value of miller indices for a specific Bragg refelction, while a and c both is lattice parameter. A small difference was seen in the value of a and c for YSZ13 and YSZ14 compared to YSZ15, which was reflected by the change in bond distance during the heating process (19). Besides, the lattice parameter was calculated after confirming the tetragonal structure according to the existence of peak at (101), (002) and (110). Therefore, only YSZ13, YSZ14 and YSZ15 were recorded, whereby YSZ14 has the highest crystallite size. Moreover, a slightly shift peak towards the right for YSZ13 and YSZ15

was observed where YSZ14 recorded the smallest stress value. From this analysis, it can be concluded that YSZ14 or

 $1400\ ^{\circ}\mathrm{C}$  is the most optimize temperature for preparing YSZ thin film electrolyte.

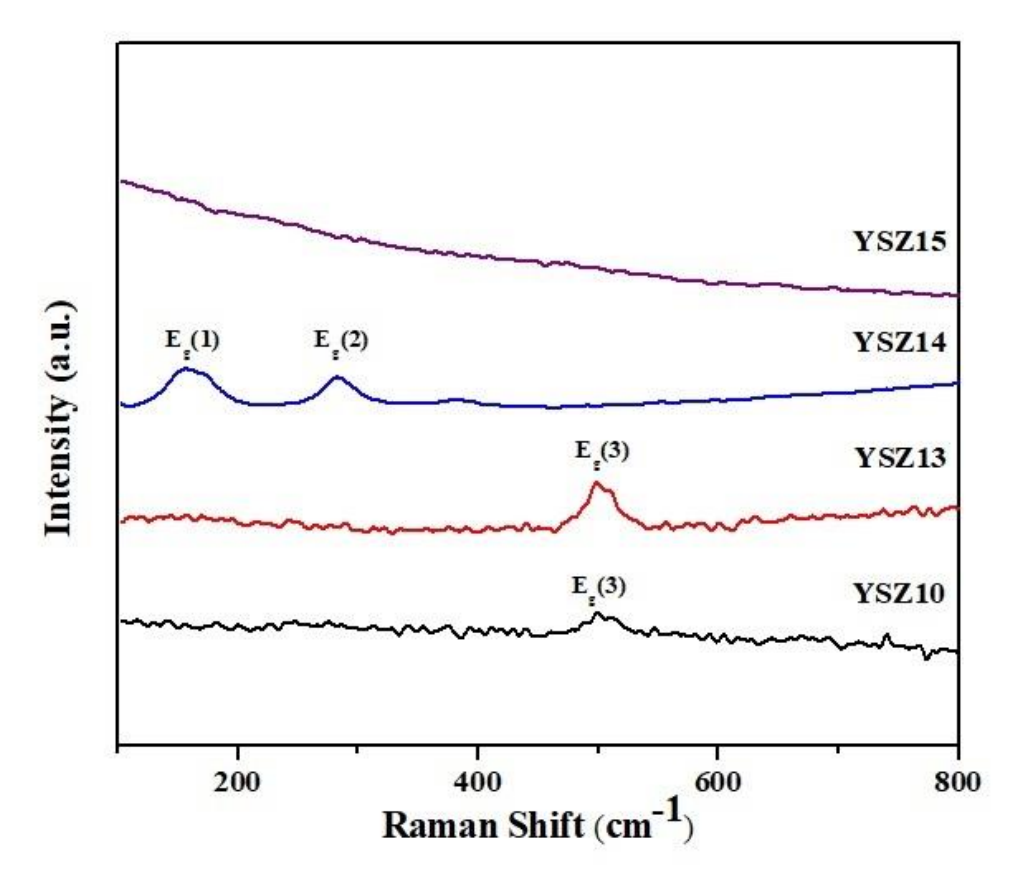


Figure 1: XRD patterns of the deposited YSZ thin films

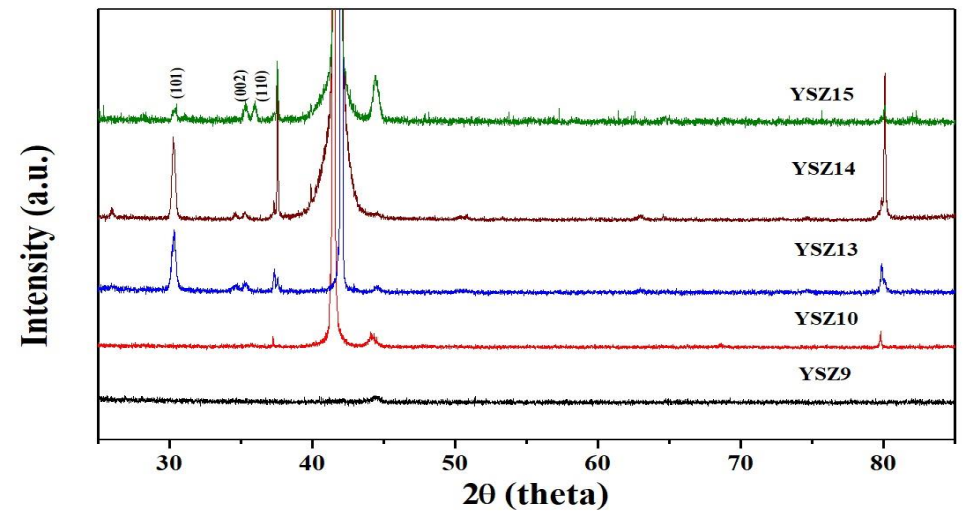


Figure 2: Magnified view corresponding to the high intensity peak (101) from XRD

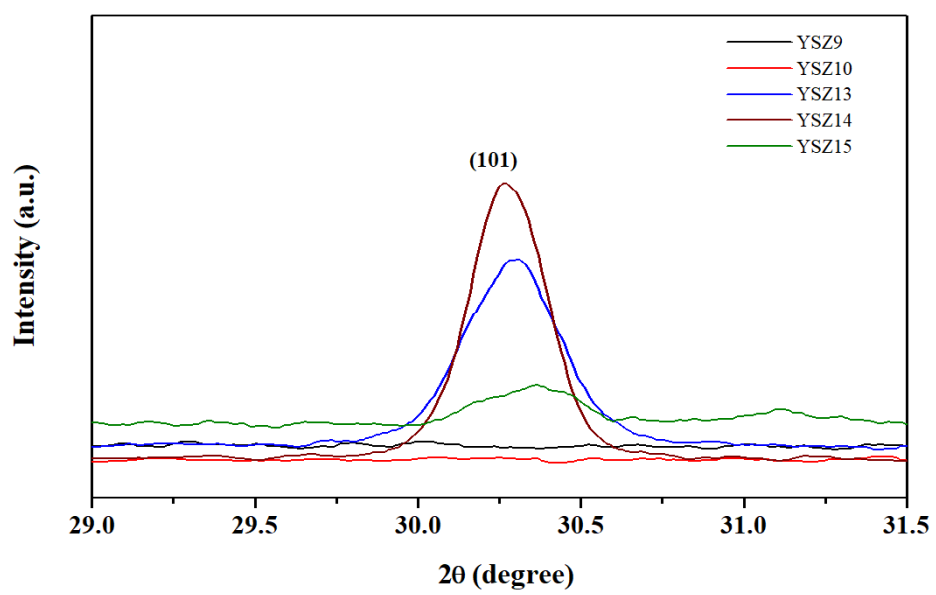


Figure 3: Raman spectra of the selected films

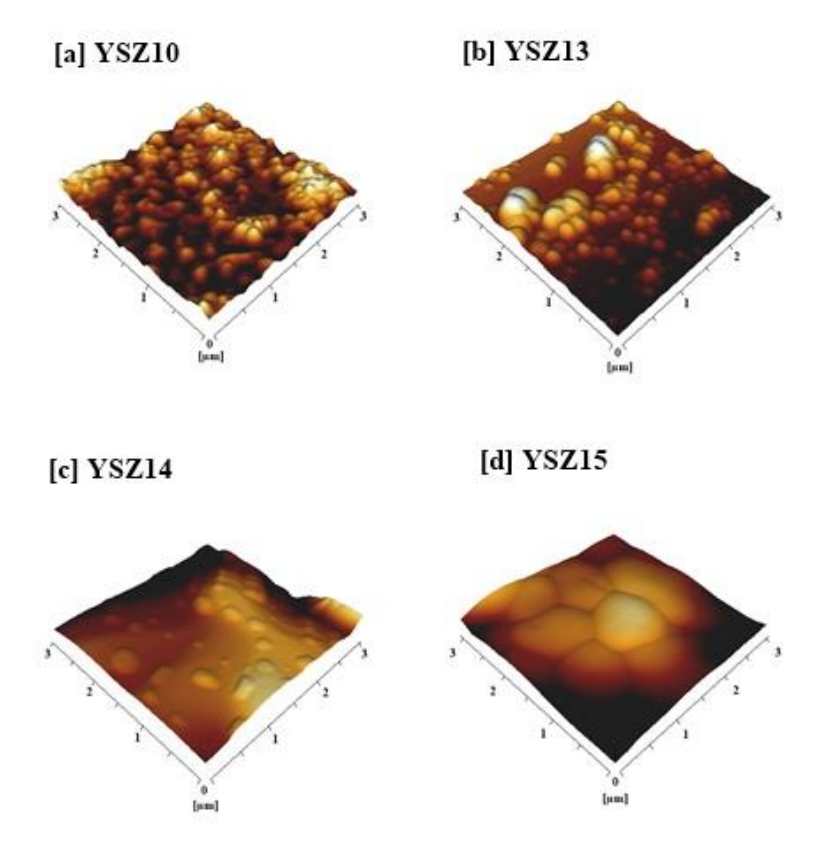


Figure 4: a) YSZ10, b) YSZ13, c) YSZ14 and d) YSZ15 are 3-Dimensional AFM

Table 1: Crystallite size, lattice strain and lattice parameter of the prepared YSZ thin films

of the prepared 152 thin thins				
Sample Code	Crystallite Size, D (nm)	Lattice Strain (nm)	Lattice Parameter	
YSZ13	24.06	0.0054	a = 3.598 c = 5.186	
YSZ14	34.55	0.0038	a = 3.601 c = 5.186	
YSZ15	31.02	0.004	a = 3.532 c = 5.068	

#### 3.2 Raman spectra

Figure 3 presents the selected Raman spectra of YSZ films sintered at 1000 °C, 1300 °C, 1400 °C and 1500 °C, whereby the samples are denoted as YSZ10, YSZ13, YSZ14 and YSZ15, respectively. The observed Raman peaks showed three prominent peaks related to the  $E_{\rm g}$  (1),  $E_{\rm g}$  (2) and  $E_{\rm g}$  (3) symmetric vibration modes of tetragonal YSZ crystal (20). YSZ10 and YSZ13 revealed a single peak at 500 cm $^{-1}$ , depicting a tetragonal YSZ with coupled Zr-O bonding and stretching mode. The stretching mode O-Zr-O appeared at tetragonal YSZ of YSZ14 thin film at its peak of 281.91 cm $^{-1}$ . The three samples supported the XRD result in identifying the structure of the film, but YSZ15 did not show any signal at all due to some defects occurring during high temperature treatments.

### 3.3 Three-Dimensional (3D) AFM analysis

Figure 4 depicts the 3-Dimensional AFM images of the YSZ thin films. The YSZ thin films displayed homogeneous surfaces for YSZ10, YSZ13, YSZ14, and YSZ15, whereas YSZ9 was neglected due to the peak absence in the XRD pattern prior. Grain growth of the YSZ thin films could be seen in the images. By increasing the temperature, the grain boundaries were distinguished and small grains stuck together to form larger grains. The grain size of the film is calculated and shown in Table 2. It could be observed that the grain size increased with incremental sintering temperatures. Similarly, the root mean square roughness (RMS) and average roughness (Ra) were important parameters, whereby the roughness also increased as the sintering temperature increased. Even though the roughness for YSZ15 decreased from 181.1 nm to 129.4 nm, the grain size was too big to be considered. This would be important for subsequent testing and analysis, such as in terms of electrical properties in order to achieve a high performance of ionic conductivity.

Table 2: Grain size, RMS roughness and average roughness of the prepared thin film samples

	1 1		
Sample	Grain Size	RMS	Average
Code	(nm)	Roughness	Roughness, Ra
		(nm)	(nm)
7707710	122.25	1 6 0 7	20.07
YSZ10	132.25	16.87	20.87
YSZ13	209.55	25.92	42.43
YSZ14	232.47	133.6	181.1
YSZ15	995.2	100.4	129.4

## **4 Conclusions**

A series of YSZ electrolyte thin films were deposited onto the c-plane of the sapphire substrate at different sintered temperatures and the samples were characterised accordingly. The sintering temperature variation was found to significantly affect the structures and morphologies of these films. The XRD analyses showed the formation of stable crystalline structures of YSZ sintered at 1400 °C. The Raman spectra confirmed the occurrence of two prominent crystalline YSZ peaks at 1400 °C, thereby supporting the XRD observation. The morphology of the samples sintered at higher temperatures revealed highly disturbed growths with the grains merging together, roughening of surface, and size enlargements. It was worth the efforts to improve the YSZ thin film structures from tetragonal to cubic as the cubic phase was more stable. Hence, the present findings may be useful for the development of SOFCs to support the green technology for industrial developments and humanity.

## **Aknowledgments**

Authors and researchers are sincerely grateful to acknowledge the financial support from UTM and Ministry of Education through GUP Vote number Q.K1300000.2540.20H27 and FRGS 5F050.

### **Ethical issue**

Authors are aware of, and comply with, best practice in publication ethics specifically with regard to authorship (avoidance of guest authorship), dual submission and manipulation of the figures, competing interests, and the compliance with policies on research ethics. Authors adhere to publication requirements that submitted work is original and has not been published elsewhere in any language.

# **Competing interests**

The authors declare that there is no conflict of interest that would prejudice the impartiality of this scientific work.

# Authors' contribution

All authors of this study have a complete contribution for data collection, data analyses and manuscript writing

#### References

- Salleh SF, Gunawan MF, Zulkarnain MF Bin, Shamsuddin AH, Abdullah TART. Modelling and optimization of biomass supply chain for bioenergy production. J Environ Treat Tech. 2019;7(4):689–95.
- Lee TD, Ebong AU. A review of thin film solar cell technologies and challenges. Renew Sustain Energy Rev. 2017; 70:1286–97.
- Choudhury A, Chandra H, Arora A. Application of solid oxide fuel cell technology for power generation - A review. Renew Sustain Energy Rev. 2013;20:430–42.
- Hoveidi H, Aslemand A, Borhani F, Naghadeh SF. Emission and Health Costs Estimation for Air pollutants from Municipal Solid Waste Management Scenarios, Case Study: NO x and SO x Pollutants, Urmia, Iran. J Environ Treat Tech. 2017;5(1):59–64.
- Stambouli AB, Traversa E. Solid oxide fuel cells (SOFCs): a review of an environmentally clean and efficient source of

- energy. 2002;6:433-55.
- Noh H-S, Son J-W, Lee H, Song H-S, Lee H-W, Lee J-H. Low Temperature Performance Improvement of SOFC with Thin Film Electrolyte and Electrodes Fabricated by Pulsed Laser Deposition. J Electrochem Soc. 2009;156(12):B1484.
- Mahato N, Banerjee A, Gupta A, Omar S, Balani K. Progress in material selection for solid oxide fuel cell technology: A review. Prog Mater Sci. 2015;72:141–337.
- Manoharan D, Loganathan A, Kurapati V, Nesamony VJ. Unique sharp photoluminescence of size-controlled sonochemically synthesized zirconia nanoparticles. Ultrason Sonochem. 2015;23:174–84.
- Barelli L, Barluzzi E, Bidini G. Diagnosis methodology and technique for solid oxide fuel cells: A review. Int J Hydrogen Energy. 2013;38(12):5060–74.
- Hedayat N, Du Y, Ilkhani H. Review on fabrication techniques for porous electrodes of solid oxide fuel cells by sacri fi cial template methods. Renew Sustain Energy Rev. 2017;77(August 2016):1221–39.
- Badwal SPS, Foger K. Solid oxide electrolyte fuel cell review. Ceram Int. 1996;22(3):257–65.
- 12. Kisi EH, Howard CJ. Crystal structures of zirconia phases and their inter-relation. Key Eng Mater. 1998;154(153–154):1–36.
- 13. Jacobson AJ. Materials for Solid Oxide Fuel Cells †. Chem Mater Rev. 2010;660–74.
- Navrotsky A. Thermochemical insights into refractory ceramic materials based on oxides with large tetravalent cations. J Mater Chem. 2005;15(19):1883.
- Viazzi C, Bonino JP, Ansart F, Barnabé A. Structural study of metastable tetragonal YSZ powders produced via a sol-gel route. J Alloys Compd. 2008;452(2):377–83.
- Figueiredo FML, Marques FMB. Electrolytes for solid oxide fuel cells. Wiley Interdiscip Rev Energy Environ. 2013;2(1):52–72.
- 17. Changrong X, Huaqiang C, Hong W, Pinghua Y, Guangyao M, Dingkun P. Sol-gel synthesis of yttria stabilized zirconia membranes through controlled hydrolysis of zirconium alkoxide. J Memb Sci. 1999;162(1–2):181–8.
- 18. Singhal SC. SOLID OXIDE FUEL CELLS: AN OVERMEW. 2004;49:999–1000.
- Talebi T, Haji M, Raissi B, Maghsoudipour A. YSZ electrolyte coating on NiO-YSZ composite by electrophoretic deposition for solid oxide fuel cells (SOFCs). Int J Hydrogen Energy. 2010;35(17):9455-9.
- Heiroth S, Frison R, Rupp JLM, Lippert T, Barthazy Meier EJ, Müller Gubler E, et al. Crystallization and grain growth characteristics of yttria-stabilized zirconia thin films grown by pulsed laser deposition. Solid State Ionics. 2011;191(1):12–23.